Electronic Supplementary Material (ESI) for Journal of Materials Chemistry B.

Supplementary Information

Studying the capture efficiency of small extracellular vesicles using magnetic beads coated with tannic acid

Nikita A. Grishaev[a], Ekaterina O. Moiseeva[a], Vasiliy S. Chernyshev[b], Aleksei S. Komlev[c], Anton M. Novoselov[d], Alexey M. Yashchenok[a]

[a]Skoltech Center for Photonic Science and Engineering, Skolkovo Institute of Science and Technology Skolkovo Innovation Center, 121205 Moscow, Russia

[b]National Medical Research Center for Obstetrics, Gynecology and Perinatology Named after Academician V.I. Kulakov, 117997 Moscow, Russia

[c]Faculty of Physics, Lomonosov Moscow State University, 119991 Moscow, Russia

[d]Department of Chemistry, Lomonosov Moscow State University, 119991 Moscow, Russia

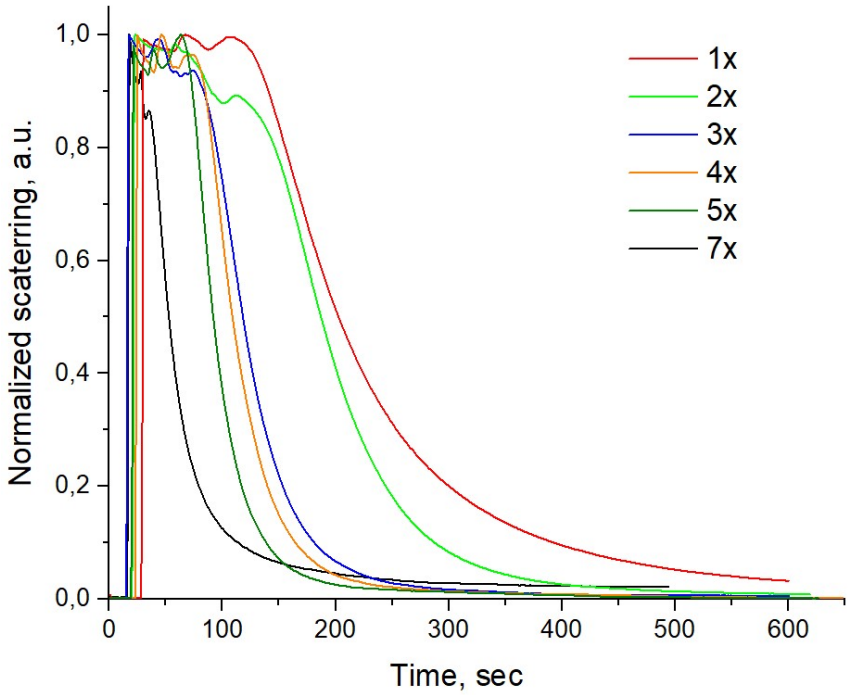

Fig. S1. Normalized scattering of MB prepared for different FIL loadings depending on time in an external magnetic field.

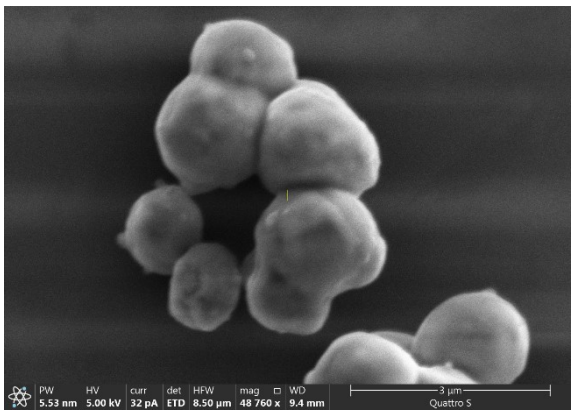

Fig. S2. SEM image of $CaCO_3$@Fe_3O_4-$(PVP/TA)_3$.

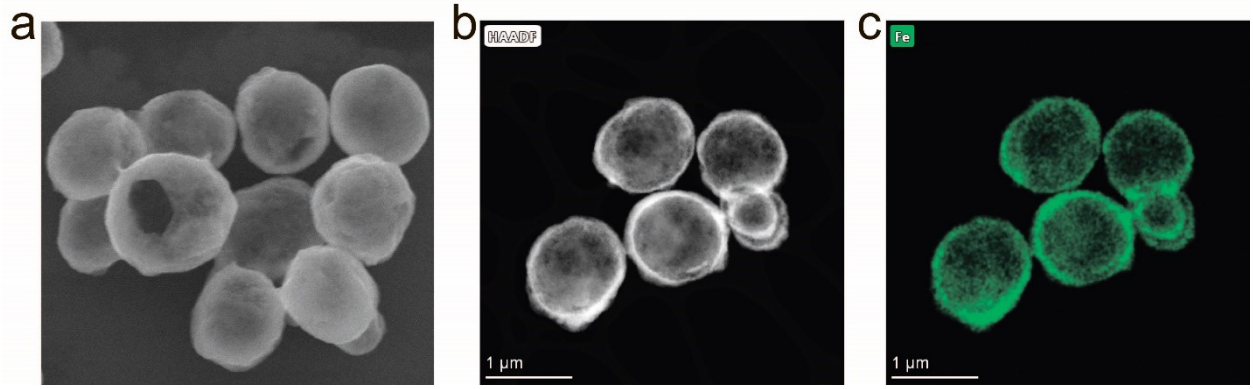

Fig. S3. SEM, HAADF-STEM, and STEM-EDS elemental mappings for TAMB-1 after decomposition of $CaCO_3$.

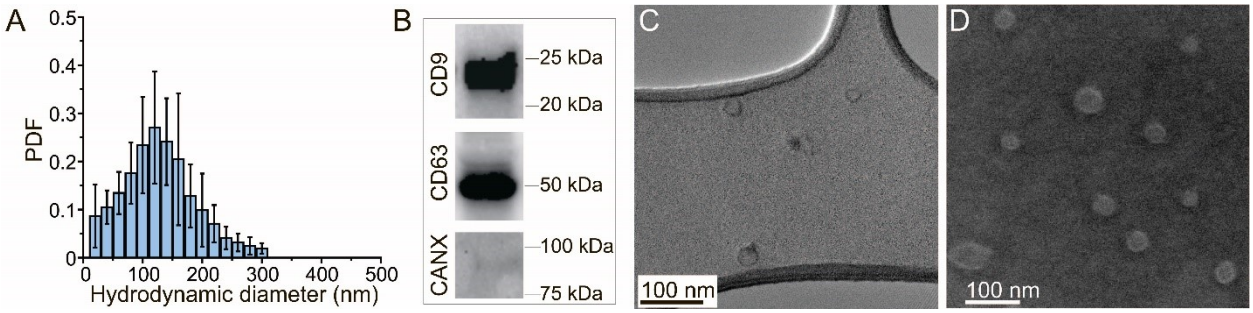

Fig. S4. (A) Hydrodynamic size distribution of sEVs isolated from MCF7 cell line determined by the NTA method. (B) Western blot of isolated MCF7 sEVs with relative expression of CD63, CD9 and absence of Calnexin. (C, D) HRTEM and SEM images of dehydrated MCF7 sEVs.

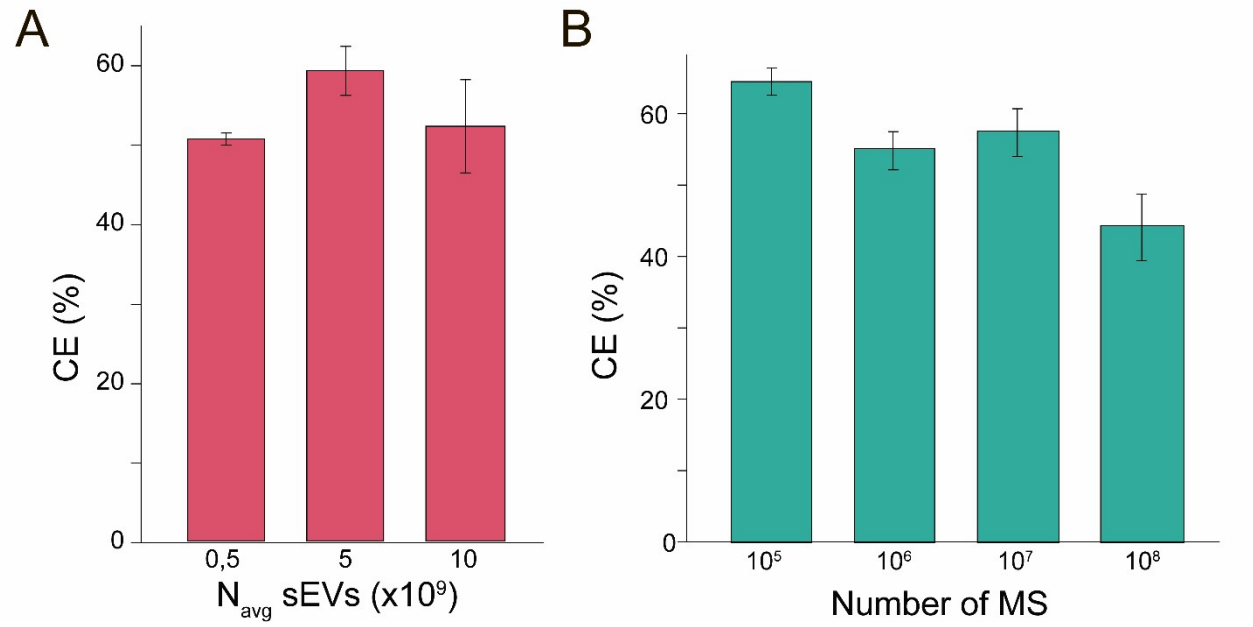

Fig. S5. (A) Capture efficiency (CE) of MCF7 sEVs to TAMB-1 depending on the concentrations of sEVs added. (B) CE of MCF7 sEVs to TAMB-1 by varying the number of TAMB-1.

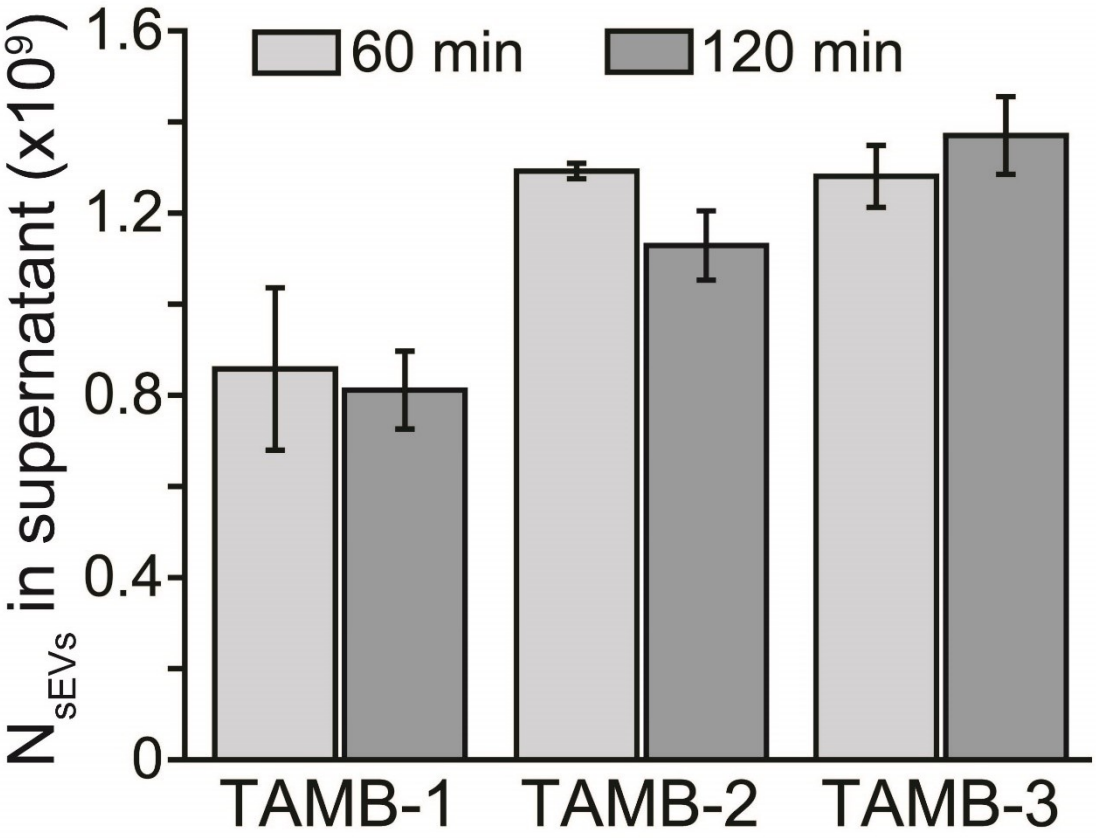

Fig. S6. Number of MCF7 sEVs determined in the supernatant by the NTA method for TAMB1, TAMB2 and TAMB3 after their incubation with sEVs during 60 and 120 min.

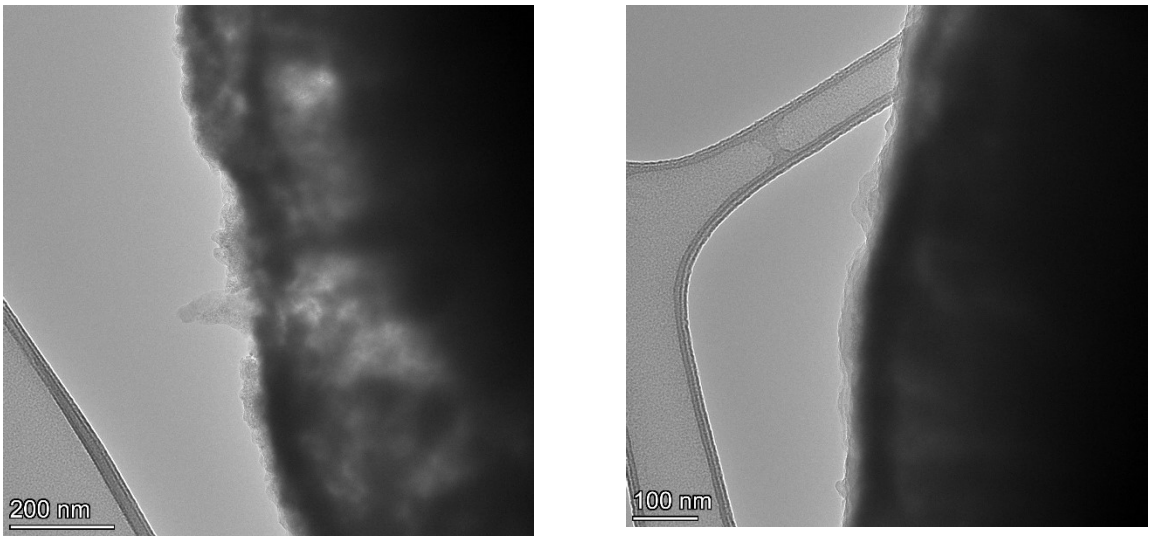

Fig S7. HRTEM images of TAMB3.

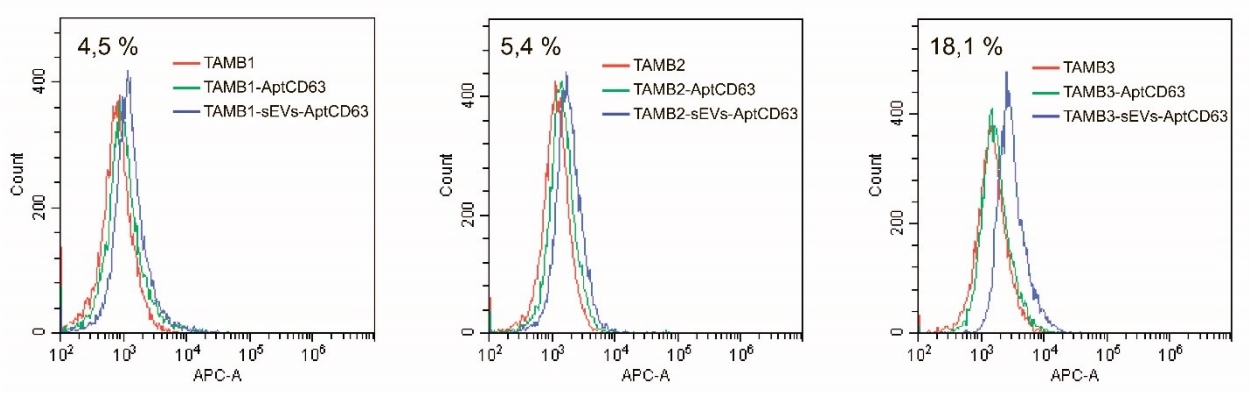

Fig. S8. Flow cytometry data of specific binding of Cy5-labeled anti-CD63 aptamer to HCT116 sEVs adsorbed on TAMB1, TAMB2 and TAMB3 (blue curves). TAMB1, TAMB2 and TAMB3, which were not incubated with HCT116 sEVs, before (red curves) and after incubation with Cy5-labeled anti-CD63 aptamer (green curves) were used as a control.

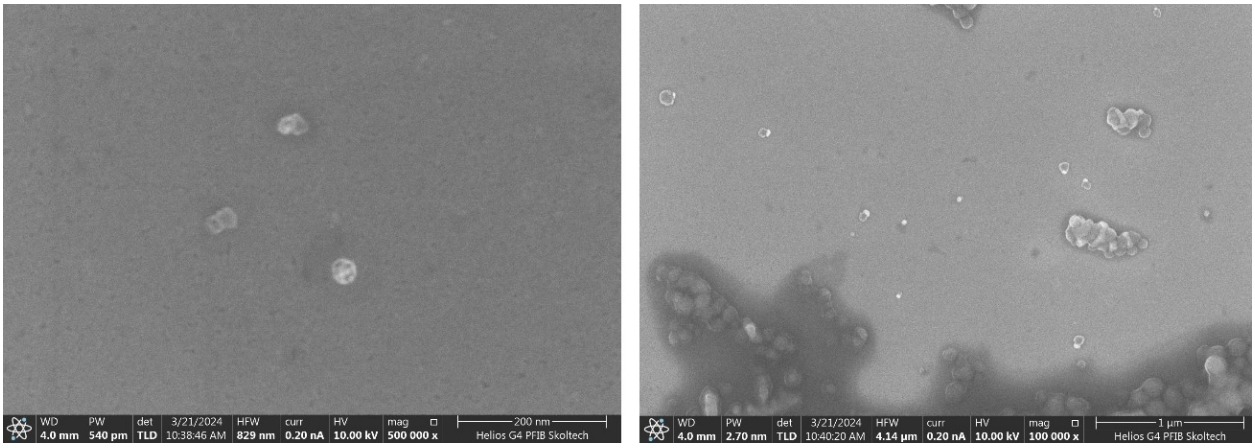

Fig. S9. SEM images of HCT116 sEVs isolated from cell culture supernatant by TAMB approach after the detachment of sEVs from TAMB using 0,1 % Tween20.

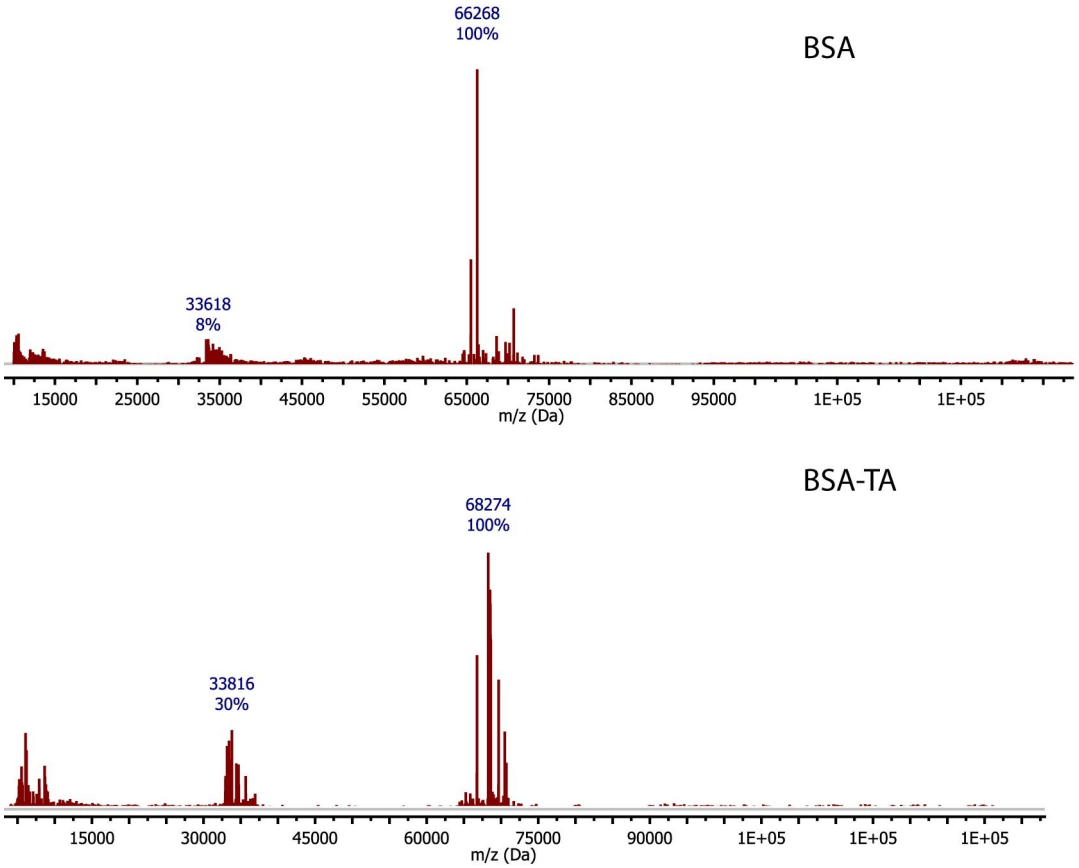

Fig. S10. MALDI-TOF mass spectra of BSA (top) and BSA-TA complex (bottom).

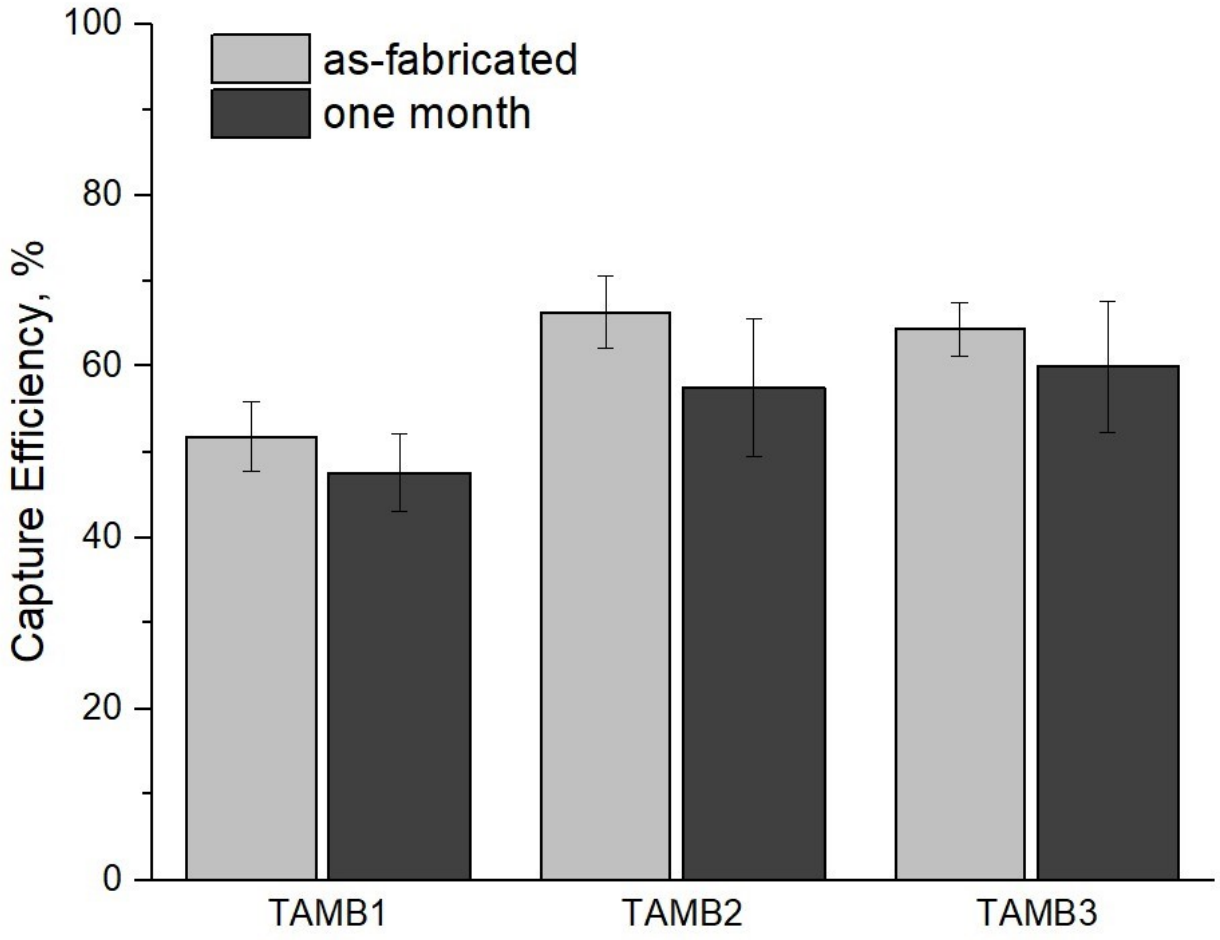

Fig. S11. Capture efficiency of MCF7 and HTC116 sEVs to TAMB1, TAMB2 and TAMB3 for freshly fabricated beads and for beads after one-month storage in the fridge.

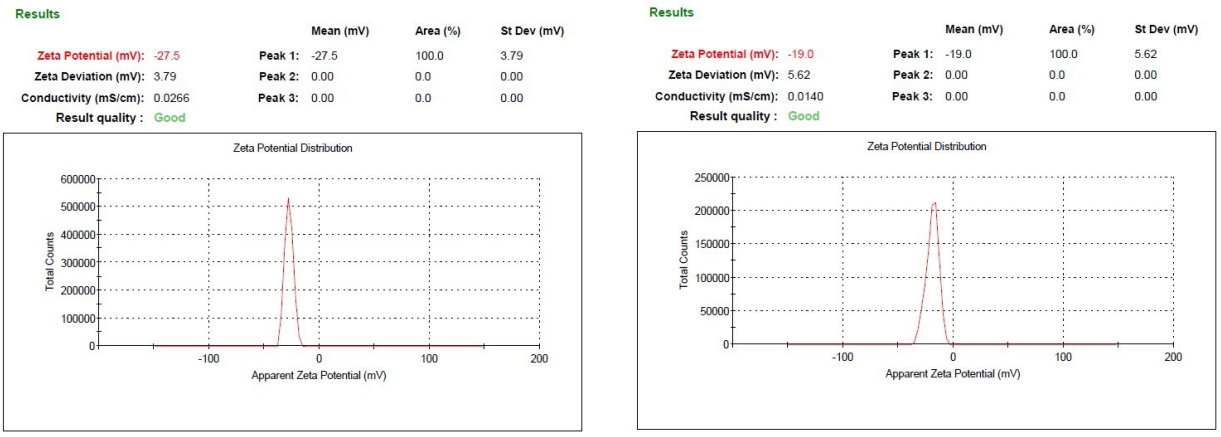

Fig. S12. Zeta-potential measurements of as-fabricated TAMB1 and TAMB1 stored for at least six months in the fridge.

References

1. German, S.V., Novoselova, M.V., Bratashov, D.N. et al. High-efficiency freezing-induced loading of inorganic nanoparticles and proteins into micron- and submicron-sized porous particles. Sci Rep 8, 17763 (2018).
2. D.V. Volodkin, A.I. Petrov, M. Prevot, G.B. Sukhorukov Matrix Polyelectrolyte Microcapsules: New System for Macromolecule Encapsulation Langmuir 2004, 20, 8, 3398-3406.
3. B.V. Parakhonskiy, A. Haase, R. Antolini Sub-Micrometer Vaterite Containers: Synthesis, Substance Loading, and Release Angew. Chem. Int. Ed. 2012, 51, 1195-1197.
4. German, S.V., Inozemtseva, O.A., Markin, A.V. et al. Synthesis of magnetite hydrosols in inert atmosphere. Colloid J 75, 483-486 (2013).
5. https://tetraquant.com/products
6. V.S. Chernyshev, D. Nozdriukhin, R. Chuprov-Netochin, E. Tsydenzhapova, M. Novoselova, D. Gorin, A. Yashchenok Engineered multicompartment vesicosomes for selective uptake by living cells Colloids and Surfaces B: Biointerfaces 220 (2022) 112953.
7. A.M. Yashchenok, V.S. Chernyshev, E.V. Konovalova, R. Kholodenko, E. Tsydenzhapova, V.O. Shipunova, A.A. Schulga, S.M. Deyev, D.A. Gorin AntiCD63Oligonucleotide Functionalized Magnetic Beads for the Rapid Isolation of Small Extracellular Vesicles and Detection of EpCAM and HER2 Membrane Receptors using DARPin Probes Analysis&Sensing, 2022, e202200059